Results in Engineering 16 (2022) 100707

Contents lists available at ScienceDirect

Results in Engineering

journal homepage: www.sciencedirect.com/journal/results-in-engineering

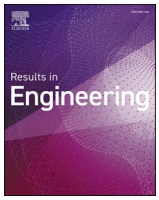

The effect of electron beam irradiation and fillers on natural rubber prepared by latex mixing: A Small and Wide Angle X-ray scattering study

Worawat Jansomboon [a], Sirinart Chio-Srichan [b], Surapich Loykulnant [c], Paweena Prapainainar [a,d,*]

[a] National Center of Excellence for Petroleum, Petrochemicals and Advance Material, Department of Chemical Engineering, Faculty of Engineering, Kasetsart University, Bangkok, 10900, Thailand
[b] Synchrotron Light Research Institute (Public Organization), 111 University Avenue, Suranaree, Muang District, Nakhon Ratchasima, 30000, Thailand
[c] National Metal and Materials Technology Center, 114 Thailand Science Park, Phaholyothin Rd, Klong 1, KlongLuang, PathumThani, 12120, Thailand
[d] Department of Chemistry and NANOTEC Center for Nanoscale Materials Design for Green Nanotechnology, Kasetsart University, Bangkok, 10900, Thailand

ARTICLE INFO

Keywords:
Natural rubber
Electron beam irradiation
Graphene nanoplatelets
Small angle X-ray scattering (SAXS)
Wide angle X-ray scattering (WAXS)
Synchrotron

ABSTRACT

The natural rubber (NR) cured by electron beam (EB) irradiation prepared by latex mixing was studied via small angle and wide angle x-ray scattering (SAXS and WAXS) techniques for the first time. In this study, the effect of EB irradiation doses (100–250 kGy) and fillers (graphene nanoplatelets (GE), mixture of silica and graphene nanoplatelets (TSi/20%GE) on the mean distance of crosslink and strain-induced crystallization were investigated. The SAXS experiments revealed that the maximum position of the plot (qmax) was increased from 1.76 nm to 1 to 1.99 nm-1, indicating that the mean distance between crosslinks of NR decreased due to the occurrence of crosslink networks after EB irradiation processes. It was found that the mean distance between crosslinks of all EB-irradiated NR was insignificantly different (q_{max} ~ 1.94–1.99 nm^{-1}) although the higher crosslink density was found in NR with the higher EB dose. Likewise, the addition of fillers did not also affect the mean distance between crosslinks of NR. The discussion led to the conclusion that the mean distance of NR depended on the type of crosslink networks. The WAXS study revealed that the intensities of crystallinity reflection peaks increased in the function of EB irradiation dose. It can be seen in all NR types that molecular chains of NR were still in amorphous regions although the high stretching was applied. Additionally, the crystallinity percentage of EB-irradiated NR in stretching mode was always lower than that in retraction mode, which the highest crystallinity percentage was found in the case of NR250 (41.89% crystallinity at 500% strain). Based on WAXS results, the conclusions were in agreement with NR cured by other vulcanization systems. Finally, it was found that addition of TSi/20%GE in NR pulled down the level of strain – induced crystallization, which the crystallinity percentage was 27.75% at 500% strain, while the crystallinity percentage of NR added GE was 36.19% at the same strain.

1. Introduction

Numerous products used in everyday life of humans are made of natural rubber (NR). Its excellent properties such as tensile and elastic properties were the main reason why NR has been applied for many applications [1]. It can also be mixed with nanomaterials to enhance product properties [2–4]. One of the outstanding characteristics of NR is strain – induced crystallization, which is the phenomenon that the crystallinity of NR increased due to the ordered molecular chains of NR during stretching, resulting in reinforcement itself [5]. The strain – induced crystallization is still a popular subject for NR research although it has been discovered for almost 100 years [6].

The strain – induced crystallization and crystallinity during deformation condition of NR has been investigated and observed by X-ray diffraction and reported in many works [7–9]. Specifically, small angle and wide angle x-ray scattering (SAXS and WAXS) techniques were also widely applied for the studies of NR molecular structure both static and dynamic experiments. Influential factors such as cure temperature [10],

* Corresponding author. Department of Chemical Engineering, Faculty of Engineer, Kasetsart University, 50 Ngamwongwan Road, Ladyao, Jatujak, Bangkok, 10900, Thailand.
E-mail addresses: worawat.ja@ku.th (W. Jansomboon), sirinart@slri.or.th (S. Chio-Srichan), surapicl@mtec.or.th (S. Loykulnant), fengpwn@ku.ac.th (P. Prapainainar).

https://doi.org/10.1016/j.rineng.2022.100707
Received 28 June 2022; Received in revised form 14 October 2022; Accepted 15 October 2022
Available online 22 October 2022

impurities concentration [11], ratio of blending [12], filler type and concentration [13], endlinking network and entanglement [14], vulcanizing agents [15], sulphur crosslink types [16], were studied in depth-details in order to evaluate the effect on strain – induced crystallization of NR. Additionally, the effect of the vulcanization system was reported in previous works. For example, the behavior of orientation of molecular chain and strain - induced crystallization of NR cured by sulphur and peroxide was investigated by in-situ synchrotron equipment. The results demonstrated that there was no significant difference of these subjects between NR vulcanizates [17]. There were also some publications reporting the difference between microscopic structure of NR and other rubber types such as isoprene rubber [18]. However, the behavior of strain – induced crystallization of NR vulcanized by irradiation such as electron beam (EB) has not been studied enough. The related studies of irradiated NR were rare and have never been widely reported, especially by the implementation of X-ray diffraction experiment.

A new technology which has been applied for polymer modification – including NR vulcanization – is EB irradiation. The exposure of high energy originated from EB radiation established crosslink networks of molecular chains occurring after stimulated intermediates such as free radicals and ions joined and created new bonds with others [19]. A strong point of the irradiation technique is that the crosslinking degree of the materials can be controlled and by adjusting the exposure time and the electron accelerator in order to obtain the optimum properties of the desired material. Furthermore, the benefit from the absence of chemical substances and curing agents involved with the irradiation processes enhanced the advantages of EB irradiation for NR modification [20]. Many publications have reported the studies of the applications of EB irradiation in several NR styles such as neat NR [21–23], epoxidized NR [24], NR blends [25,26], grafted NR [27], NR foam (Salmazo at al., 2016), NR filled with fillers (Jansomboon 2019b; [28–30]. According to these works, the improvement of material properties such as mechanical and thermal properties are found by the effect of EB irradiation.

The strain – induced crystallization of NR cured by sulphur and peroxide vulcanization were studied by the technique of X-ray scattering and reported elsewhere. However, the elucidation of the behavior of strain – induced crystallization of NR cured by EB irradiation have not been proposed. In this paper, the effect of EB irradiation and fillers added into NR, including crystallization behavior were studied by SAXS and WAXS. Uncured NR (neat NR) and cured NR (EB-irradiated NR at various doses, and EB-irradiated NR filled with graphene nanoplatelets (GE) and the mixture of silica and graphene nanoplatelets (TSi/20%GE)) were irradiated by EB irradiation for vulcanization. All types of NR samples were kept at latex condition during irradiation. The effect of EB irradiation doses and fillers on the molecular chains of NR and its behavior under stretching were investigated by SAXS and WAXS. Finally, the discussion of the results compared with other vulcanization systems were presented.

2. Experimental

2.1. Materials and chemical substances

High-ammonia concentrated latex included 62% of dry rubber was provided by the National Science and Technology Development Agency (Thailand). Graphene nanoplatelets (specific area of 500 m^2/g) were obtained from Alfa Aesar company (USA). Silicon dioxide (specific area of 163 m_2/g) was given by Grand Chemical Far East Ltd (Thailand). All chemical substances used for silica surface treatment which were ethanol (99.9%) and TESPTS (98%) were given by Sigma-Aldrich (USA).

2.2. Preparation of EB-irradiated NR

All types of desired NR samples needed to be primarily prepared from the neat NR latex before the next steps. First, 40 g of high-ammonia concentrated latex (HA natural rubber) composed of 62% of dry rubber which was provided by the National Science and Technology Development Agency (Thailand) was weighed and transferred to small plastic boxes. In cases of EB-irradiated NR filled with fillers, 2.5 phr of the mixture of silica and graphene nanoplatelets (TSi/20%GE) or 2.5 phr of individual graphene nanoplatelets (GE) were added in NR matrix via magnetic stirrer mixing at 500 rpm for 30 min. The procedures of these mixtures preparation can be seen in Ref. [28]. These plastic boxes contained NR compounds were then moved to the irradiation area which was the 80 × 80 cm^2 aluminum tray. The room temperature was maintained during the irradiation process. The EB irradiation doses were varied as 100, 150, 200, and 250 kGy, carried out by the electron beam accelerator (Model: MB10-50). The conveyor speed at the process dose of 50 kGy was 1.299 m/min, which the setting of the electron accelerator machine was 10 MeV. The EB-irradiated NR products were rapidly casted onto a 0.1 cm-thick mirror plate and kept for 12 h before drying at 55 °C in an automatic incubator for 3 h. The dried NR samples were kept in zip-lock plastic bags and preserved in the dark to avoid moisture and sunlight. The summarized details of all NR samples were presented in Table 1.

Table 1
The details of all NR samples.

Sample code	Vulcanization by EB irradiation	EB irradiation doses (kGy)				Addition of filler	Filler types
		100	150	200	250		
NR0	–					–	
NR100	✓	✓				–	
NR150	✓		✓			–	
NR200	✓			✓		–	
NR250	✓				✓	–	
NR/GE	✓		✓			✓	GE
NR/Tsi/20% GE	✓		✓			✓	TSi/20% GE

2.3. Scanning electron microscope (SEM)

The morphology of cross-sectional surface of EB-irradiated NR was studied using a FEI QUANTA 450 scanning electron microscope. The desired surfaces selected for investigation were obtained by breaking NR samples in liquid nitrogen.

2.4. Test of crosslink density

Swelling of EB-irradiated NR was tested by immersing a small rectangular NR sample in toluene at room temperature for 3 days. The weight difference before and after immersing was determined. Then, it was used for crosslink density calculation implemented in the same method as described elsewhere [31]. The crosslink density of EB-irradiated NR was calculated based on the Flory-Rehner equation as follows [32–35].

$$V_c = \rho_p [N_A / M_A] \quad (A)$$

where V_c is the crosslink density of the NR sample, ρ_p is the density of natural rubber (0.915 g/cm^3), N_A is Avogadro's number (6.02 × 10^{23} mol^{-1}), and M_A is the average molecular weight of crosslinked NR.

2.5. SAXS and WAXS experiments

The SAXS and WAXS experiments were carried out at the beamline BL1.3W: SAXS/WAXS (Small and Wide Angle X-ray Scattering), the Siam Photon Laboratory, Synchrotron Light Research Institute, Nakhon Ratchasima, Thailand. The photon energy of 9 keV (equivalent to the wavelength of 0.138 nm) was selected using a double multilayer

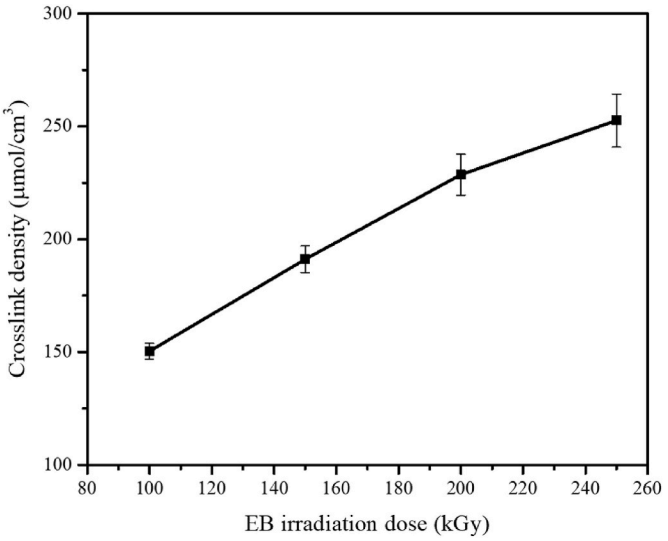

Fig. 1. Crosslink density of EB-irradiated NR varied at 100, 150, 200, and 250 kGy.

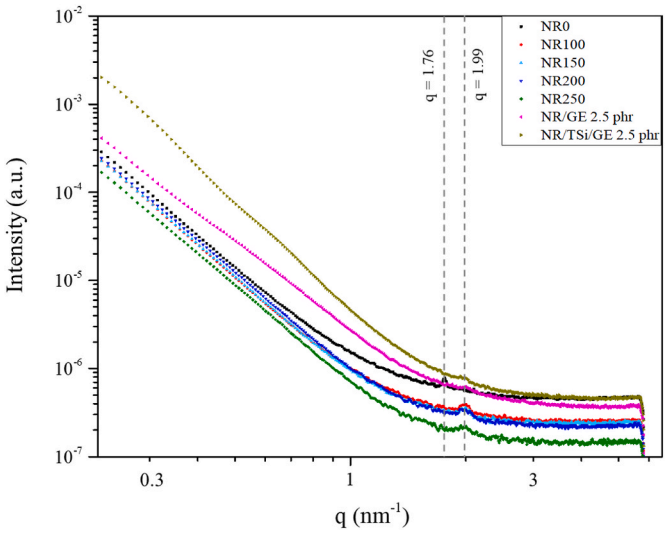

Fig. 2. SAXS profiles for uncured NR (NR0), NR irradiated at 100–250 kGy (NR100, NR150, NR200, NR250), NR irradiated at 150 kGy filled 2.5 phr of GE (NR/GE 2.5 phr), and NR irradiated at 150 kGy filled 2.5 phr of TSi/20%GE (NR/TSi/20%GE 2.5 phr).

monochromator (W/B4C). For SAXS experiment, a small piece of NR sample was deposited on a metal sample frame with the size of 10 × 10 mm and placed on the sample stage. A CCD camera, Rayonix SX165 was used to capture the scattering profiles of the samples. The experiment was carried out in air. The exposure time of the X-ray was 600 s.

The mean distance was calculated from SAXS experiment. According to Ref. [36]; the mean distance between scattering center (ξ) can be calculated from an equation of

$$\xi = (2\pi)/(q\_max)$$

where q_{max} is the maximum position of scattering vector q.

In the case of the WAXS experiment, a dumbbell-shaped NR sample was horizontally mounted to the grips of an in-situ tensile equipment provided by SCG chemical group, Thailand. The temperature of the tensile stage was fixed at 0 °C during stretching and retraction. The tensile stage was stopped for each desired strain point – the fixed strain stretching (0, 100, 200, 300, 400, and 500%) and the fixed strain retraction (400, 300, 200, 100, and 0%) to collect the static WAXS pattern and data. The speed of deformation applied for the NR sample was 10 mm/s. The scattering patterns and data were recorded using a Rayonix LX170HS detector. The experiments were performed in air. The exposure time of the X-ray was 90 s.

The SAXS and WAXS data and patterns were analyzed using the developed in-house Matlab-based data processing program called SAXSIT (V.4.47). The crystallinity percentages of each NR type during deformation were also determined by fitting crystalline reflection peaks method with pseudo-voigt peak fitting method for WAXS data.

3. Results and discussion

3.1. Crosslink density

Data from the swelling experiment carried out by immersing NR sample in toluene for 3 days were used for crosslink density calculation. According to equation *A*, crosslink density of EB-irradiated NR with 100–250 kGy were plotted and shown in Fig. 1. As expected, it can be seen that crosslink density of EB-irradiated NR increased when dose of EB increased. The highest crosslink density was found in NR irradiated at 250 kGy which was about 250 μmol/cm^3. The reason might be that reaching more energy from higher EB irradiation dose caused an increase in crosslinking structure of NR molecular chain. However, a large variation of crosslink density of NR irradiated at high EB doses could be found due to the effect of chain scission reaction. This result was generally found in publications involved with rubber modified by irradiation such as the work of [29,31].

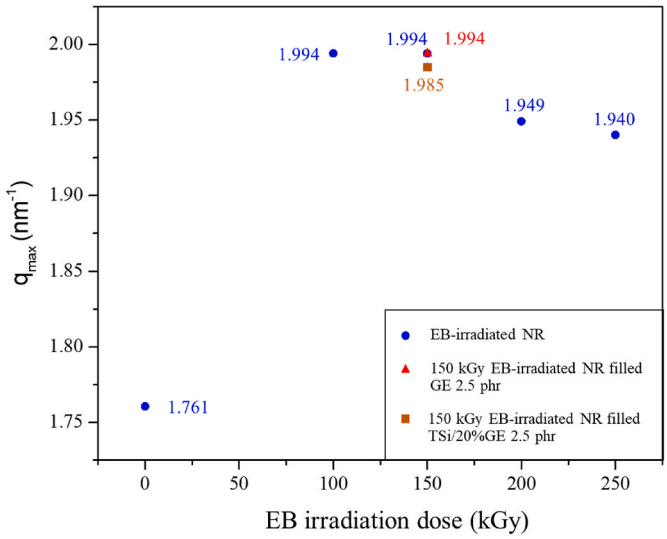

Fig. 3. q_{max} as a function of EB irradiation dose for uncured NR and EB-irradiate NR.

3.2. SAXS results

The SAXS intensity I(q) against the scattering vector q for all NR samples are plotted in a log scale and shown in Fig. 2. The maximum position of the plot (q_{max}) as a function of EB irradiation dose for uncured NR and EB-irradiated NR are also shown in Fig. 3. It can be seen that q_{max} from the uncured NR (NR0) was ~1.76 nm^{-1}. After EB irradiation, q_{max} of NR increased which were ~1.99 nm^{-1} for NR irradiated at 100 and 150 kGy (NR100 and NR150, respectively). It is widely known that the high irradiation energy can be applied for crosslink and curing in elastomer materials such as NR. q_{max} were likely to decrease when the increase in EB dose to 200 and 250 kGy applied for NR, which was ~1.95 for NR200 and ~1.94 for NR250. It might be due to an

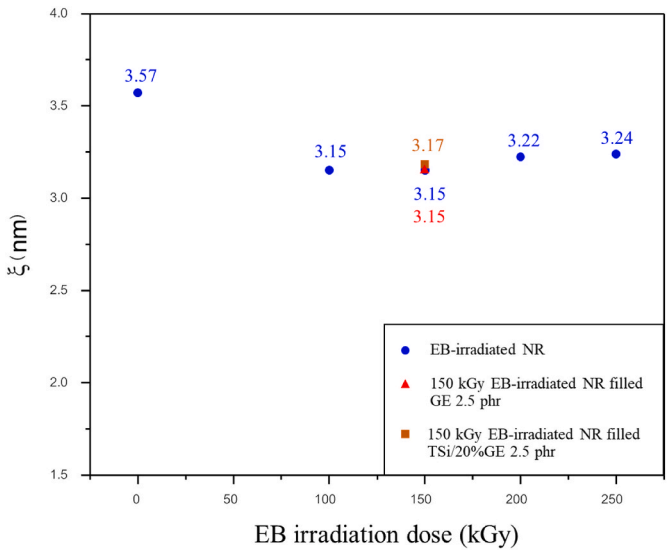

Fig. 4. Mean distance between crosslinks as a function of EB irradiation dose applied for NR vulcanization.

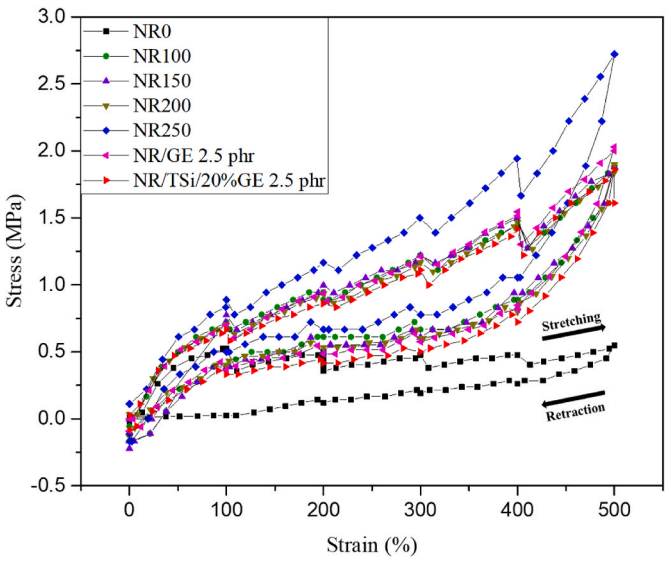

Fig. 5. Stress – strain curve of uncured NR and EB-irradiated NR indicating both stretching and retraction mode.

increase in chain scission reaction in a high dose of EB irradiation, which small chain scission fragments were generated instead of suitable crosslink network [31]. However, the difference of q_{max} between these EB-irradiated NR was very small when compared to the difference of q_{max} between uncured and cured NR by irradiation. q_{max} of EB-irradiated NR filled 2.5 phr of GE and TSi/20%GE (NR/GE and NR/TSi/GE, respectively) were also insignificantly different from q_{max} of NR150, indicating that addition of these fillers at the concentration of 2.5 phr into irradiated NR matrix rarely affected on q_{max} of irradiated NR at the same EB dose. A reason might be that the size of filler particles used in this study were in micro scale.

Furthermore, the features of SAXS profiles of NR samples can be explained by Porod scattering. The scattering patterns display power law decays in intensity which can be defined as $1/Q^P$, where P is the power law exponent or Porod parameter. This parameter can be used to describe the geometry and interface roughness of the sample. The data in Fig. 2 were fitted with straight lines with R-squared of 0.99. We observe the scattering profiles at the high q, with the power law decay $\sim 1/Q^4$ suggesting smooth surface structure in NR/TSi/GE sample while which of other NR and NR/GE decay $\sim 1/Q^3$ suggesting rough surface structure [37]. The reason might be that the surface of the NR composite is rather smooth when there are TSi fillers in the composite.

The difference of q_{max} between uncured NR and EB-irradiated NR observed in Fig. 3 was due to occurrence of C–C crosslinked network of NR molecular chain after exposure of EB irradiation. The mean distance between scattering center ξ (it can be called crosslinks in this study related to NR) are shown in Fig. 4. As expected, the decrease in the mean distance between crosslinks in NR was the result of the increase in crosslink network in NR matrix due to EB irradiation, which ξ of NR0 showed the value of 3.57 nm, while ξ of NR100 and NR150 showed the value of 3.15 nm. The explanation should be that because the reduction of the distance between NR molecular chains occurred when NR exposed the high energy of irradiation and crosslink occurred. However, a slight increase in ξ was found when the level of EB doses was increased, representing a value of 3.22 nm for NR200 and 3.24 nm for NR250. The possible reason should be that many fragmentations of NR chain due to chain scission reactions occurred competitively with the reaction of crosslink network at high level of EB irradiation dose [31,38]. Therefore, it might be said that too much intensity of irradiation increased in the mean distance between crosslinks in NR.

Additionally, the mean distance of NR irradiated at 150 kGy filled 2.5 phr of GE (NR/GE 2.5 phr), and NR irradiated at 150 kGy filled 2.5 phr of TSi/20%GE (NR/TSi/20%GE 2.5 phr) showed an insignificant difference from the mean distance of unfilled NR150, indicating that addition of fillers into NR matrix did not affect on the mean distance between crosslink of NR composites, according to the SAXS results.

The finding in this study was different from a previous work reported that the mean distance between crosslinks of NR increased after curing NR by sulphur vulcanization at 400 K [10]. The reason might be due to the difference curing system. In the vulcanization system by irradiation – as presented in this study – the formation of crosslink was C–C which would give a result in packing of molecular chains. On the other hand, in the case of sulphur vulcanization system, many sulfides crosslinks and sulphidic groups occurred during the crosslink process. These bulky sulphur structures provided a result of increase in the mean distance between crosslinks. Additionally, it was found that the mean distance of EB-irradiated NR in this work (~3.2 nm) was lower than that of sulphure-vulcanized NR (~4.5 nm). Therefore, it can be concluded that the mean distance ξ of NR depended on the type of crosslink networks occurred in the system after curing processes. Additionally, it might be claimed that the mean distance between crosslink of EB-irradiated NR is shorter than that of sulphure-vulcanized NR.

3.3. WAXS results

The stress-strain curve and collection of WAXS patterns of all EB-irradiated NR during being applied stress which the samples were held at the fixed strain stretching (0, 100, 200, 300, 400, and 500%) and the fixed strain retraction (400, 300, 200, 100, and 0%) under the speed of 10 mm/s of deformation and the temperature of 0 °C are shown in Figs. 5–6. Although the stress relaxation behavior could be found at all point of fixed strain for all EB-irradiated NR samples due to the holding, it is obvious that the strength of EB-irradiated NR composited was the function of EB irradiation dose, which – in this study – NR irradiated at 250 kGy (NR250) showed the highest stress at all strain. The increase in stress of polymer composites as a function of irradiation dose was generally found in many publications [31,39,40]. The stress of retraction of NR samples was also lower than which of stretching due to the hysteresis loss.

In Fig. 6, it can be clearly seen that there was indifference to the WAXS pattern of all NR samples. The beginning of oriented crystalline reflection peaks shows at a stretching strain of 200%. When the stretching strain of the samples was increased, the intensities of peaks of crystalline reflection increased. As expected, the greatest intensities of

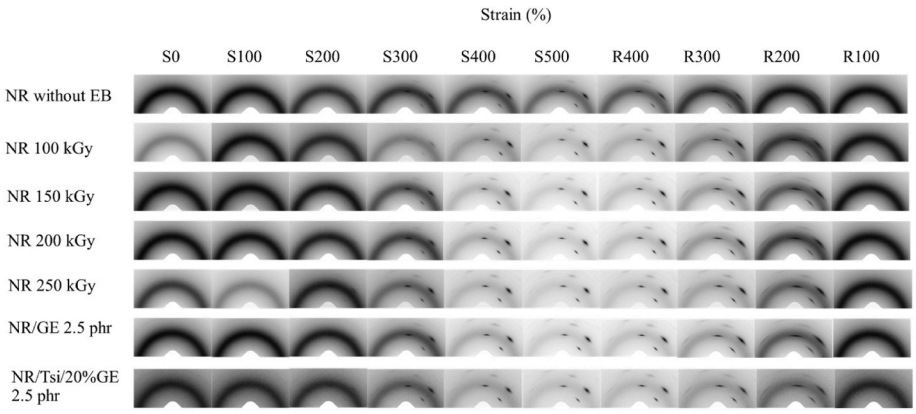

Fig. 6. The collected WAXS pattern of each NR types at various strains both stretching and retraction. Strain – induced crystallization of NR during deformation.

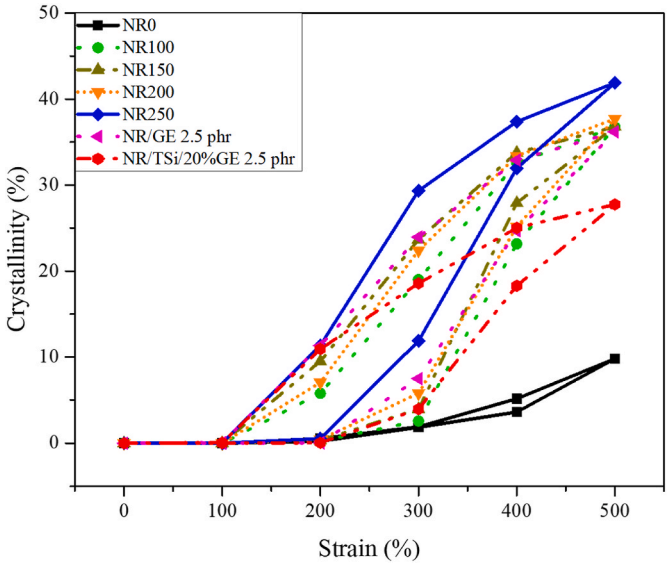

Fig. 7. The crystallinity percentage during stretching and retraction of each NR types under the speed of 10 mm/s of deformation.

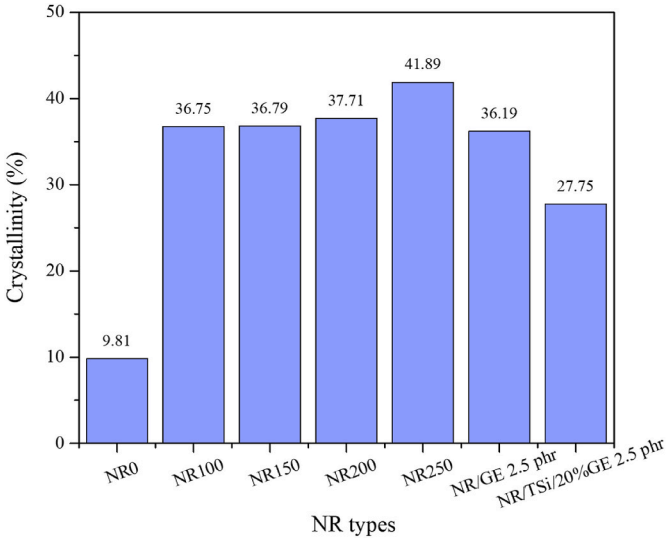

Fig. 8. The crystallinity percentage at 500% strain of each NR type.

crystalline reflection patterns were observed when the stretching strain was maximum. On the other hand, during retraction, the intensities of these patterns decreased when the strain of the samples was decreased, which no any crystalline pattern can be seen in the strain at 0 and 100%. The crystal structure appeared in this study based on WAXS pattern is in accordance with a system of monoclinic unit cell, which Bunn (1947) reported the parameter of polyisoprene unit cell: $a = 1.25$ nm, $b = 0.89$ nm, c (chain axis) $= 0.81$ nm, and $\beta = 92°$.

The WAXS patterns of each EB-irradiated NR samples also show that – when comparing at the same strain – the appearance of crystalline diffraction pattern of stretching mode is less than that of retraction mode. For example – not only this case but also another case in the same manner – the crystalline pattern of NR samples at the retraction of 200 % strain (R200) is greater and clearer than that of NR sample at the stretching of 200%strain (S200). The above phenomenon is due to hysteresis effect which is consistent with the stress – strain testing, and generally observed in NR.

Additionally, it was found that the crystalline patterns of NR cured by EB irradiation and their behavior observed in this study were not different from the crystalline patterns of NR cured by sulphur [41,42] and peroxide [17]. Numerous crosslink network in these cured NR molecular chain resulted in an effective strain-induced crystallization occurred during stretching. Therefore, it might be claimed that the crystalline patterns of NR were not disparate by exposure of EB irradiation.

The crystallinity percentages of each NR type during deformation were determined by fitting crystalline reflection peaks with pseudo-voigt peak fitting function for WAXS data processed using SAXSIT program. The crystallinity percentage during deformation both stretching and retraction are shown in Fig. 7, and the crystallinity percentage at 500% strain is shown in Fig. 8. Strain – induced crystallization can be seen in NR0 during stretching and retraction despite low crosslink density. Typically, the crystallinity percentages of all NR types were firstly determined at the stretching strain of 200%, which was the point that the crystallinity reflection peaks began to appear in WAXS patterns. The crystallinity percentage of NR increased when the stretching strain was increased. It reached the maximum value at 500% strain, and then decreased in the returning. It is worth noting that the crystallinity percentage in stretching mode was always lower than that in retraction mode due to hysteresis effect. The crystallinity became zero when the retraction strain was 100%, which no any reflection peaks appeared. It might be due to the reason that the induced crystallization is completely reversible at this condition.

To compare between uncured NR (NR0) and all EB-irradiated NR, it was found that the crystallinity percentage of NR0 was not significantly different from those of NR cured by EB irradiation at low strain (less than 300% strain). However, at the stretching point higher than 400% strain, the crystallinity percentage of NR0 was quite lower than that of

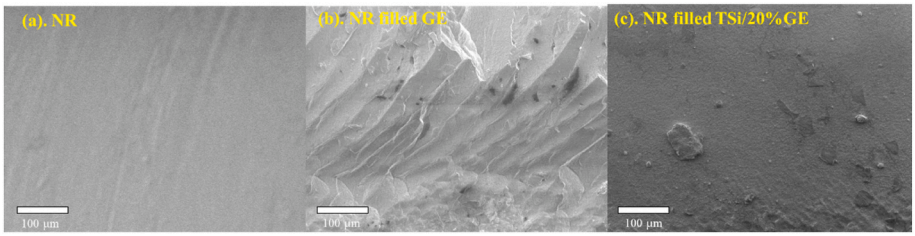

Fig. 9. SEM images of EB-irradiated NR and NR composites filled with fillers.

NR cured by EB irradiation. For example, the crystallinity percentage of NR0 at 500% stretching strain was 9.81%, while that of NR250 at the same strain was 41.89%. The explanation might be that the amorphous regions in NR0 were still large at the high stretching strains. Lack of crosslink network in NR molecular chain of NR0 resulted in an ineffective strain-induced crystallization occurred during stretching.

Additionally, it can be clearly seen that the crystallinity percentage during deformation of EB-irradiated NR increased when the level of EB doses increased. This was consistent with the above discussed result indicating that the crosslink density of NR was a function of EB doses. The higher crosslink density was, the greater strain-induced crystallization would be, indicating the greater crystallinity percentage. From these reasons, it could be explained why NR250 showed the highest crosslink density, stress, and strain – induced crystallization.

The behavior of strained – induced crystallization of irradiated NR in this work harmonized with the behavior of strained – induced crystallization of NR cured by peroxide in the work of [17]. It was reasonable to compare because the type of crosslink network in these NR vulcanizates was similarly (C–C bond). In the works of [17]; the crystallinity percentage of NR cured by peroxide at 500% strain was about 17%, while the crystallinity percentages of all EB-irradiated NR in this study at the same strain were not less than 36%. The difference between the percentage of crystallinity indicated above might be because of the inequality of crosslink density and the stretching rate in the experiment. The higher crosslink density and the stretching rate were, the greater percentage of crystallinity would be.

Types of fillers would give a different effect on the occurrence of strain-induced crystallization. In Figs. 7–8, to compare among NR150, NR/GE, and NR/TSi/20%GE, it was found that the crystallinity percentages of NR150 and NR/GE were insignificantly different, while the crystallinity percentage of NR/TSi/20%GE was obviously seen to be lower than those two NRs. The reason should be that large particles of silica and agglomerated fillers might obstruct the orientation of NR molecular chains during stretching, resulting in the low amount of crystalline region. On the other hands, the strain-induced crystallization of NR did not be significantly affected by addition of graphene nanoplatelets. It was in agreement with a previous report indicating that the negative effect of addition of low amounts of graphene on the orientation of NR molecular chains was not found (Xing et al., 2013). Therefore, it might be concluded that the strain – induced crystallization of EB-irradiated NR could be affected by adding TSi/20%GE, while adding GE in NR matrix did not affect the strain – induced crystallization of EB-irradiated NR.

3.4. Morphology

Morphology of EB-irradiated NR, NR filled GE, and NR filled TSi/20%GE which all samples were irradiated at 150 kGy are shown in Fig. 9. It can be seen that the surface of NR was quite smooth, while there were particles spread out on the surface of NR filled GE and NR filled $TSiO_2$/20%GE. A large particle and agglomeration can be found in NR/TSi/20%GE. However, there was rare agglomeration shown on the surface of NR filled with GE which was in consistent with a previous work [28], indicating a good distribution of GE on NR surface. It is worth noting that the appearance of all samples from SEM is inconsistent with the results from Porod scattering indicated in previous sections because the observation is in different scale. For example, the smooth surface structure is found in NR/TSi/GE sample by Porod parameter while filler particles can be observed from SEM image.

4. Conclusions

The SAXS experiments revealed that the mean distance between crosslinks of NR decreased after EB irradiation processes, which the value changed from 3.57 nm to about 3.15 mm due to the appearance of crosslink networks. Although the higher EB irradiation dose was, the greater crosslink density would be, it was found that the mean distance between crosslinks of EB-irradiated NR varied EB dose in the range of 100–250 kGy was insignificantly different. The addition of GE or TSi/20%GE into EB-irradiated NR did not also affect the mean distance between crosslinks of NR. The inconsistent results between irradiated NR and sulphur-cured NR [10] showed that the mean distance of NR depended on the type of crosslink networks occurring in the curing process.

The strain – induced crystallization of NR during stretching and retraction was investigated by WAXS experiments with in-situ stretching equipment. It can be clearly seen that the intensities of crystallinity reflection peaks appearing in WAXS pattern increased when the doses of EB irradiation increased, conforming to the crosslink density results. The similar behaviors of all NR in this study were observed and demonstrated that molecular chains of NR were still in amorphous regions although the high stretching was applied. It was found that the highest crystallinity percentage was reached at the largest stretching strain, which the highest value was found in the case of NR250 (41.89% crystallinity at 500% strain). Additionally, the crystallinity percentage in stretching mode was always lower than that in retraction mode. The low crystallinity percentage of NR/TSi/20%GE also indicated that the strain – induced crystallization of EB-irradiated NR could be affected by types of filler added into NR matrix.

Credit author statement

Worawat Jansomboon: Methodology, Validation, Formal analysis, Investigation, Resources, Writing - Original Draft, **Sirinart Srichan**: Review & Editing, Investigation, Visualization, Supervision, **Surapich Loykulnant**: Conceptualization, Funding acquisition, Supervision, **Paweena Prapainainar**: Conceptualization, Validation, Writing - Review & Editing, Visualization, Visualization, Supervision, Project administration.

Declaration of competing interest

The authors declare that they have no known competing financial interests or personal relationships that could have appeared to influence the work reported in this paper.

Data availability

No data was used for the research described in the article.

Acknowledgements

The authors gratefully acknowledge financial support from a grant from Thailand Research Fund (Grant No. MRG5980252) and the Thailand Graduate Institute of Science and Technology (TGIST) (Grant No. TG-33-11-58-045D). Thanks are also due to the National Center of Excellence for Petroleum, Petrochemicals, and Advanced Materials, the Faculty of Engineering at Kasetsart University, Kasetsart University Research Development Institute (KURDI), and Research Network of NANOTEC-KU on NanoCatalysts and NanoMaterials for Sustainable Energy and Environment. All technical support during SAXS/WAXS experiment from BL1.3W: SAXS′ staff are very appreciated. The author would like to thank Dr. Wonchalerm Rungswang, Thai Polyethylene Co., Ltd., Siam Cement Group (SCG), Thailand for the permission to use the in-situ tensile machine in our experiments.

References

[1] H. Mooibroek, K. Cornish, Alternative sources of natural rubber, Appl. Microbiol. Biotechnol. 53 (2000) 355–365, https://doi.org/10.1007/s002530051627.
[2] A.A. Beni, H. Jabbari, Nanomaterials for environmental applications, Results Eng 15 (2022), 100467, https://doi.org/10.1016/j.rineng.2022.100467.
[3] R. Chollakup, S. Seuthao, P. Suwanruji, J. Boonyarit, W. Smitthipong, Mechanical properties and dissipation energy of carbon black/rubber composites. Compos, Adv. Mater. 30 (2021) 1–6, https://doi.org/10.1177/26349833211005476.
[4] R. Nandee, M.A. Chowdhury, A. Shahid, N. Hossain, M. Rana, Band gap formation of 2D materialin graphene: future prospect and challenges, Results Eng 15 (2022), 100474, https://doi.org/10.1016/j.rineng.2022.100474.
[5] J.-M. Chenal, C. Gauthier, L. Chazeau, L. Guy, Y. Bomal, Parameters governing strain induced crystallization in filled natural rubber, Polymer 48 (2007) 6893–6901, https://doi.org/10.1016/j.polymer.2007.09.023.
[6] K. Loos, A.B. Aydogdu, A. Lion, M. Johlitz, J. Calipel, Strain-induced crystallisation in natural rubber: a thermodynamically consistent model of the material behaviour using a multiphase approach, Continuum Mech. Therm. 32 (2020) 501–526, https://doi.org/10.1007/s00161-019-00859-y.
[7] B. Huneau, Strain-induced crystallization of natural rubber: a review of X-ray diffraction investigations, Rubber Chem. Technol. 84 (2011) 425–452, https://doi.org/10.5254/1.3601131.
[8] S. Toki, T. Fujimaki, M. Okuyama, Strain-induced crystallization of natural rubber as detected real-time by wide-angle X-ray diffraction technique, Polymer 41 (2000) 5423–5429, https://doi.org/10.1016/S0032-3861(99)00724-7.
[9] S. Toki, The effect of strain-induced crystallization (SIC) on the physical properties of natural rubber (NR), in: K.S., I.Y. (Eds.), Chemistry, Manufacture, and Applications of Natural Rubber, Elsevier, Cambridge, 2014, pp. 135–167, https://doi.org/10.1533/9780857096913.1.135.
[10] W. Salgueiro, A. Somoza, I. Torriani, A.J. Marzocca, Cure temperature influence on natural rubber—a small angle X-ray scattering study, J. Polym. Sci. B Polym. Phys. 45 (2007) 2966–2971, https://doi.org/10.1002/polb.21293.
[11] S. Toki, C. Burger, B.S. Hsiao, S. Amnuaypornsri, J. Sakdapipanich, Y. Tanaka, Multi-scaled microstructures in natural rubber characterized by synchrotron X-ray scattering and optical microscopy, J. Polym. Sci. B Polym. Phys. 46 (2008) 2456–2464, https://doi.org/10.1002/polb.21578.
[12] W. Salgueiro, A. Somoza, A.J. Marzocca, I. Torriani, M.A. Mansilla, A SAXS and swelling study of cured natural rubber/styrene-butadiene rubber blends, J. Polym. Sci. B Polym. Phys. 47 (2009) 2320–2327, https://doi.org/10.1002/polb.21828.
[13] B. Ozbas, S. Toki, B.S. Hsiao, B. Chu, R.A. Register, I.A. Aksay, D.H. Adamson, Strain-induced crystallization and mechanical properties of functionalized graphene sheet-filled natural rubber, J. Polym. Sci. B Polym. Phys. 50 (2012) 718–723, https://doi.org/10.1002/polb.23060.
[14] S. Amnuaypornsri, S. Toki, B.S. Hsiao, J. Sakdapipanich, The effects of endlinking network and entanglement to stress–strain relation and strain-induced crystallization of un-vulcanized and vulcanized natural rubber, Polymer 53 (2012) 3325–3330, https://doi.org/10.1016/j.polymer.2012.05.020.
[15] L. Chen, X. Guo, Y. Luo, Z. Jia, J. Bai, Y. Chen, D. Jia, Effect of novel supported vulcanizing agent on the interfacial interaction and strain-induced crystallization properties of natural rubber nanocomposites, Polymer 148 (2018) 390–399, https://doi.org/10.1016/j.polymer.2018.06.058.
[16] W. Sainumsai, K. Suchiva, S. Toki, Influence of sulphur crosslink type on the strain-induced crystallization of natural rubber vulcanizates during uniaxial stretching by in situ WAXD using a synchrotron radiation, Mater. Today Proc. 17 (2019) 1539–1548, https://doi.org/10.1016/j.matpr.2019.06.179.
[17] S. Toki, I. Sics, S. Ran, L. Liu, B.S. Hsiao, Molecular orientation and structural development in vulcanized polyisoprene rubbers during uniaxial deformation by in situ synchrotron X-ray diffraction, Polymer 44 (2003) 6003–6011, https://doi.org/10.1016/S0032-3861(03)00548-2.
[18] T. Karino, Y. Ikeda, Y. Yasuda, S. Kohjiya, M. Shibayama, Nonuniformity in natural rubber as revealed by small-angle neutron scattering, small-angle X-ray scattering, and atomic force microscopy, Biomacromolecules 8 (2007) 693–699, https://doi.org/10.1021/bm060983d.
[19] A.G. Chmielewski, M. Haji-Saeid, S. Ahmed, Progress in radiation processing of polymers, Nucl. Instrum. Methods Phys. Res. B 236 (2005) 44–54, https://doi.org/10.1016/j.nimb.2005.03.247.
[20] K. Makuuchi, *An Introduction to Radiation Vulcanization of Natural Rubber Latex.* Bangkok, Thailand, T.R.I Global Co., Ltd., 2003, ISBN 9749140346.
[21] I. Banik, A.K. Bhowmick, Effect of electron beam irradiation on the properties of crosslinked rubbers, Radiat. Phys. Chem. 58 (2000) 293–298, https://doi.org/10.1016/S0969-806X(99)00371-0.
[22] W. Jansomboon, S. Loykulnant, P. Prapainainar, Electron beam radiation crosslinking of natural rubber prepared by latex mixing filled silica-graphene blend, Key Eng. Mater. 803 (2019) 361–365, https://doi.org/10.4028/www.scientific.net/KEM.803.361.
[23] W. Smitthipong, M. Nardin, J. Schultz, K. Suchiva, Adhesion and self-adhesion of rubbers, crosslinked by electron beam irradiation, Int. J. Adhesion Adhes. 27 (2007) 352–357, https://doi.org/10.1016/j.ijadhadh.2006.09.010.
[24] C.T. Ratnam, M. Nasir, A. Baharin, K. Zaman, The effect of electron beam irradiation on the tensile and dynamic mechanical properties of epoxidized natural rubber, Eur. Polym. J. 37 (2001) 1667–1676, https://doi.org/10.1016/S0014-3057(01)00011-8.
[25] E.L. Chong, I. Ahmad, H.M. Dahlan, I. Abdullah, Reinforcement of natural rubber/high density polyethylene blends with electron beam irradiated liquid natural rubber-coated rice husk, Radiat. Phys. Chem. 79 (2010) 906–911, https://doi.org/10.1016/j.radphyschem.2010.02.011.
[26] R. Manshaie, S.N. Khorasani, S.J. Veshare, M.R. Abadchi, Effect of electron beam irradiation on the properties of natural rubber (NR)/styrene–butadiene rubber (SBR) blend, Radiat. Phys. Chem. 80 (2011) 100–106, https://doi.org/10.1016/j.radphyschem.2010.08.015.
[27] T. Khamplod, S. Loykulnant, C. Kongkaew, P. Sureeyatanapas, P. Prapainainar, Electron beam radiation grafting of styrene on natural rubber using Taguchi's design, Polymer 79 (2015) 135–145, https://doi.org/10.1016/j.polymer.2015.10.016.
[28] W. Jansomboon, P. Prapainainar, S. Loykulnant, P. Kongkachuichay, P. Dittanet, P. Kumnorkaew, R.J. Young, Raman spectroscopic study of reinforcement mechanisms of electron beam radiation crosslinking of natural rubber composites filled with graphene and silica/graphene mixture prepared by latex mixing, Composites Part C: Open Access 3 (2020), 100049, https://doi.org/10.1016/j.jcomc.2020.100049.
[29] V. Phetarporn, S. Kongkaew, A. Seubsai, P. Prapainainar, Composite properties of graphene-based materials/natural rubber vulcanized using electron beam irradiation, Mater. Today Commun. 19 (2019) 413–424, https://doi.org/10.1016/j.mtcomm. 2019.03.007.
[30] C. Sukthawon, P. Dittanet, P. Saeoui, S. Loykulnant, P. Prapainainar, Electron beam irradiation crosslinked chitosan/natural rubber -latex film: preparation and characterization, Radiat. Phys. Chem. 177 (2020), 109159, https://doi.org/10.1016/j.radphyschem.2020.109159.
[31] W. Jansomboon, S. Loykulnant, P. Kongkachuichay, P. Dittanet, P. Prapainainar, Electron beam radiation curing of natural rubber filled with silica-graphene mixture prepared by latex mixing, Ind. Crop. Prod. 141 (2019), 111789. https://doi:10.1016/j.indcrop.2019.111789.
[32] I. Gelling, A. Tinker, H. Rahman, Solubility parameters of epoxidised natural rubber, J. Nat. Rubber Res. (20–29) (1991). ISSN: 0127-7065.
[33] S. Hosseini, M. Razzaghi-Kashani, On the role of nano-silica in the kinetics of peroxide vulcanization of ethylene propylene diene rubber, Polymer 133 (2017) 8–19, https://doi.org/10.1016/j.polymer.2017.10.061.
[34] I. Igwe, O. Ezeani, Studies on the transport of aromatic solvents through filled natural rubber, Int. J. Polym. Sci (2012) 1–11, https://doi.org/10.1155/2012/212507, 2012.
[35] J. Wang, S. Pan, Y. Zhang, S. Guo, Crosslink network evolution of BIIR/EPDM blends during peroxide vulcanization, Polym. Test. 59 (2017) 253–261.
[36] A. Guinier, G. Fournet, Small Angle Scattering of X-Rays, Wiley, New York, 1955.
[37] P. Pakornpadungsit, T. Prasopdee, N.M. Swainson, A. Chworos, W. Smitthipong, DNA:chitosan complex, known as a drug delivery system, can create a porous scaffold, Polym. Test. 83 (2020), 106333, https://doi.org/10.1016/j.polymertesting.2020.106333.
[38] K.S. Bandzierz, L.A. Reuvekamp, G. Przybytniak, W.K. Dierkes, A. Blume, D. M. Bieliński, Effect of electron beam irradiation on structure and properties of styrene-butadiene rubber, Radiat. Phys. Chem. 149 (2018) 14–25, https://doi.org/10.1016/j.radphyschem.2017.12.011.
[39] N. BenBettaïeb, T. Karbowiak, S. Bornaz, F. Debeaufort, Spectroscopic analyses of the influence of electron beam irradiation doses on mechanical, transport properties and microstructure of chitosan-fish gelatin blend films, Food Hydrocolloids 46 (2015) 37–51, https://doi.org/10.1016/j.foodhyd.2014.09.038.
[40] L.O. Salmazo, A. Lopez-Gil, Z.M. Ariff, A.E. Job, M.A. Rodriguez-Perez, Influence of the irradiation dose in the cellular structure of natural rubber foams cross-linked by electron beam irradiation, Ind. Crop. Prod. 89 (2016) 339–349, https://doi.org/10.1016/j.indcrop.2016.05.023.
[41] S. Murakami, K. Senoo, S. Toki, S. Kohjiya, Structural development of natural rubber during uniaxial stretching by in situ wide angle X-ray diffraction using a synchrotron radiation, Polymer 43 (2002) 2117–2120, https://doi.org/10.1016/S0032-3861(01)00794-7.
[42] S. Toki, I. Sics, S. Ran, L. Liu, B.S. Hsiao, S. Murakami, S. Kohjiya, New insights into structural development in natural rubber during uniaxial deformation by in situ

synchrotron X-ray diffraction, Macromolecules 35 (2002) 6578–6584, https://doi.org/10.1021/ma0205921.